Abstract for the 12^{th} International Workshop on Water Waves and Floating Bodies, Marseille, France, March 1997.

STEADY WAVE SYSTEMS IN A TWO-LAYER FLUID OF FINITE DEPTH

Thai Nguyen and Ronald W. Yeung
Naval Architecture and Offshore Engineering
University of California at Berkeley, Berkeley, CA 94720-1780, USA.

1. Introduction

Density stratification occurs frequently in the open oceans. Surface or sub-surface marine vehicles can operate in such an environment. This gives rise to some hydrodynamic problems of intrinsic interest. If the pycnocline thickness is small, a common model is to treat the medium as a two-layer fluid. A review of this subject indicates that existing derivations of the source potential in a two-layer fluid usually assume the lower fluid to be infinitely deep [1-3] or upper fluid bound by a rigid lid [2]. A more recent formulation [4] does allow each fluid layer to have finite depth but requires the density difference between the two layers to be small. Under this latter assumption, the surface and internal wave systems are only weakly coupled. In this paper, the translating source potential for a two-layer fluid of finite depth is derived in a form amenable to numerical evaluation. The source is restricted, for illustration purpose, to the upper layer, but the density difference between the two layers can be finite. Surface and internal wave patterns are computed for a density difference large enough so that some coupling between the surface and internal wave systems exists and their intertwined behavior is observed and illustrated.

2. Mathematical Formulation

Let's define a rectangular coordinate system moving with a point source at a constant speed U along the positive x-axis. The (x, y) plane of this system coincides with the undisturbed interface between the two fluid layers, and the z-axis is positive upward. Let ρ_1, h_1 and ρ_2, h_2 denote the densities and depths of the upper and lower layers, respectively. If the velocity potential in each layer is given by $G^{(m)}(\xi, \eta, \zeta; x, y, z)$, where (ξ, η, ζ) is the location of the source and $m = 1, 2$ refers to the upper and lower fluid layer, respectively, then the governing equations for $G^{(m)}$'s are

$$\nabla^2 G^{(1)} = \delta(x - \xi, y - \eta, z - \zeta) \qquad \nabla^2 G^{(2)} = 0 \tag{1}$$

The linearized boundary conditions on the free surface $z = h_1$, the interface $z = 0$, and the rigid bottom $z = -h_2$ are:

$$k_o G_z^{(1)} + G_{xx}^{(1)} - \mu G_x^{(1)} = 0 \qquad z = h_1 \tag{2}$$

$$\gamma(k_o G_z^{(1)} + G_{xx}^{(1)} - \mu G_x^{(1)}) = k_o G_z^{(2)} + G_{xx}^{(2)} - \mu G_x^{(2)} \qquad z = 0 \tag{3}$$

$$G_z^{(1)} = G_z^{(2)} \qquad z = 0 \tag{4}$$

$$G_z^{(2)} = 0 \qquad z = -h_2 \tag{5}$$

where $k_o = g/U^2$ and $\gamma = \rho_1/\rho_2$. The fictitious viscosity μ, introduced in the above formulation to facilitate the satisfaction of the radiation condition, will be taken to zero in the final results. Finally, the radiation or asymptotic condition is given by

$$\lim_{x \to +\infty} \sqrt{R} \nabla G^{(m)} = o(1), \qquad \lim_{x \to -\infty} \sqrt{R} \nabla G^{(m)} = O(1). \tag{6}$$

where $R = \sqrt{(x - \xi)^2 + (y - \eta)^2}$.

3. Solution of the Source Functions

The solutions for $G^{(m)}$'s are assumed to have the following forms

$$G^{(1)} = \frac{1}{r} + G_o^{(1)} \qquad G^{(2)} = G_o^{(2)} \tag{7}$$

where $r^2 = (x-\xi)^2 + (y-\eta)^2 + (z-\zeta)^2$ and $G_o^{(m)}$'s are some harmonic functions in their respective domains. Using Fourier transform, represented here by the symbol $\mathcal{F}\{\}$, we can express $\mathcal{G}_o^{(m)}(k,\theta,z) = \mathcal{F}\{G_o^{(m)}(x,y,z)\}$ as

$$\mathcal{G}_o^{(m)}(k,\theta,z) = A^{(m)}(k,\theta)e^{kz} + B^{(m)}(k,\theta)e^{-kz} \tag{8}$$

where $A^{(m)}$ and $B^{(m)}$ are unknown functions of k and θ. Substituting the above expression of $\mathcal{G}_o^{(m)}(k,\theta,z)$ into the Fourier transforms of Eqns. (2)-(5), and (7), we obtain a system of linear equations which can be solved for $A^{(m)}$ and $B^{(m)}$. Once $A^{(m)}$ and $B^{(m)}$ are known, $\mathcal{G}_o^{(m)}(k,\theta,z)$ can be inverted to the (x,y,z) space, and by using Eqn. (7) again, we obtain the following expressions for the $G^{(m)}$'s.

$$\begin{aligned} G^{(1)} &= \frac{1}{r} - \frac{1}{2\pi}\int_{-\pi}^{\pi}\int_0^{\infty} \{2\epsilon ab e^{-kd}\cosh[k(z-\zeta)] + 2a(a+\gamma b)e^{-kh}\cosh[k(z-\zeta)] - \epsilon b^2 e^{k(h-z-\zeta)} \\ &\quad + \epsilon a^2 e^{-k(h-z-\zeta)} - b(a+\gamma b)e^{k(d-z-\zeta)} + a(\gamma a + b)e^{-k(d-z-\zeta)}\}\frac{e^{ik\omega}}{\Delta}dkd\theta \end{aligned} \tag{9}$$

$$G^{(2)} = \frac{\gamma}{2\pi}\int_{-\pi}^{\pi}\int_0^{\infty}\{b(a+b)[e^{k(h+z-\zeta)} + e^{k(d-z-\zeta)}] - a(a+b)[e^{-k(h+z-\zeta)} + e^{-k(\delta-z-\zeta)}]\}\frac{e^{ik\omega}}{\Delta}dkd\theta$$

where $\epsilon = 1-\gamma$

$d = h_1 - h_2$ $\qquad$ $h = h_1 + h_2$

$a = k + k_o\sec^2\theta + i\mu\sec\theta$ $\qquad$ $b = k - k_o\sec^2\theta + i\mu\sec\theta$

$\omega = (x-\xi)\cos\theta + (y-\eta)\sin\theta$ $\qquad$ $\Delta(k,\theta) = 2\epsilon ab\cosh(kd) + b(\gamma a + b)e^{kh} + a(a+\gamma b)e^{-kh}$

It is possible to show that if we let h_2 in Eqn. (9) goes to infinity, we will recover the two-layer Green function for the case of infinitely deep lower fluid layer as given in [2]. In another scenario, $G^{(1)}$ and $G^{(2)}$ can be reduced to the potential of a source moving in a uniform fluid of depth h by letting $\rho_1 = \rho_2$. Alternatively, $G^{(1)}$ can be reduced to the same uniform source potential of depth h_1 when we take $\gamma = 0$, or $h_2 = 0$.

To obtain the final results for $G^{(m)}$'s, we will now take the limit of the expressions in Eqn. (9) with μ goes to zero . The θ integration in Eqn. (9) can be redefined to range from $(-\frac{\pi}{2}, \frac{\pi}{2})$ by taking advantage of some symmetry properties of the integrand. We can therefore write $G_o^{(m)}$ as

$$G_o^{(m)} = \lim_{\mu\to 0}\Re e\left\{\int_{-\frac{\pi}{2}}^{\frac{\pi}{2}}\int_0^{\infty} H^{(m)}(k,\theta)\frac{e^{ik\omega}}{\Delta}dkd\theta\right\} \tag{10}$$

where $\Re e\{\}$ represents the real part of the complex expression inside the $\{\}$, and $H^{(m)}(k,\theta)$'s are some known functions. The roots of the equation $\Delta = 0$ are of critical importance. They are given implicitly by:

$$k_n = k_o\sec^2\theta\frac{t_1 + t_2 + (-1)^{n+1}[(t_1+t_2)^2 - 4\epsilon t_1 t_2(1+\gamma t_1 t_2)]^{\frac{1}{2}}}{2(1+\gamma t_1 t_2)} - i\mu\sec\theta, \qquad n = 1,2 \tag{11}$$

where $t_1 = \tanh(k_n h_1)$, $t_2 = \tanh(k_n h_2)$. The roots k_1 and k_2 can be assigned to be associated with the surface wave mode and internal wave mode, respectively. Note that Eqn. (11) does not always yield a solution for k_n for all values of θ. A useful way of characterizing this complex relation is to define the following two critical Froude numbers Fr_1 and Fr_2 corresponds to the maximum phase velocity c_1 of the surface wave mode and c_2 of the internal wave mode, respectively:

$$Fr_n^2 = \frac{c_n^2}{gh} = \frac{1}{2} + (-1)^{n+1}\left(\frac{1}{4} - \epsilon\frac{h_1 h_2}{h^2}\right)^{\frac{1}{2}}, \qquad n = 1,2 \tag{12}$$

By definition, $Fr_2 < Fr_1$. It can be shown that when $Fr = U/\sqrt{gh} > Fr_n$, a "supercritical" case, k_n does not exist for $|\theta| < \theta_n = \cos^{-1}(Fr_n/Fr)$. By contrast, when $Fr < Fr_n$, the "subcritical" case, k_n exists for all values of θ within the range of integration. Note that $k_1 > k_2$, and as μ approaches zero, both roots approach the positive real axis from the lower half of the complex plane. The inner $(k-)$ integral of Eqn. (10) can now be evaluated using one of the contours as shown in Figs. 1 and 2 depending on whether $\omega > 0$ or $\omega < 0$ (see, e.g. [5]). In the limit of $R \to \infty$, the integrals along the path Γ_2 and Γ_4 vanish. Cauchy's residue theorem can be applied to yield:

$$G_o^{(m)} = \Re e\left\{-\int_{-\frac{\pi}{2}}^{\frac{\pi}{2}}\int_{\Gamma_3} H^{(m)}(\sigma,\theta)\frac{e^{i\sigma\omega}}{\Delta(\sigma,\theta)}d\sigma d\theta\right\} + 2\pi\sum_{n=1}^{2}\Im m\left\{\int_{-\frac{\pi}{2}}^{\frac{\pi}{2}-\psi} H^{(m)}(k_n,\theta)\frac{e^{ik_n\omega}}{\Delta'(k_n,\theta)}d\theta\right\} \tag{13}$$

where $\Delta' = \partial\Delta/\partial k$ and $\psi = \tan^{-1}[y/(-x)]$. The integrals along Γ_3 and Γ_5 are complex conjugates of each other and have been combined to obtain this final expression, which is amenable to numerical treatment. Note that when $Fr > Fr_n$, k_n does not exist for all θ, and the range of integration of the single integral should be modified accordingly. For example, if $\frac{\pi}{2} - \psi > \theta_n > 0$, the range of integration is actually $(-\frac{\pi}{2}, -\theta_n)$ and $(\theta_n, \frac{\pi}{2} - \psi)$.

4. Surface Waves and Internal Waves

The surface waves and internal waves due to a translating point source can now be calculated as follows

$$\zeta^{(1)}(x,y) = \frac{U}{g} G_x^{(1)}\Big|_{z=h_1} \qquad \zeta^{(2)}(x,y) = \frac{U}{g\epsilon}(G_x^{(2)} - \gamma G_x^{(1)})\Big|_{z=0} \tag{14}$$

If we restrict our analysis of the wave patterns to the far field of the source, then we only need to focus on the single integrals in Eqn. (13). In the far field, $\zeta^{(m)}$ can be written as

$$\zeta^{(m)}(x,y) \sim \sum_{n=1}^{2} \Re e \left\{ \int_{-\frac{\pi}{2}}^{\frac{\pi}{2}-\psi} P^{(m)}(k_n,\theta) e^{ik_n\omega} d\theta \right\} \tag{15}$$

According to Eqn. (15), both surface and internal waves contain contributions from the poles k_1 and k_2, where, as mentioned earlier, we associate the contribution from k_1 with the surface wave mode and the contribution from k_2 with the internal wave mode. The method of stationary phase can be applied to Eqn. (15) in the usual manners. The term $e^{ik_n\omega}$ can be rewritten as $e^{i\bar{R}f_n(\theta,\psi)}$, where $\bar{R} = \sqrt{(x-\xi)^2 + (y-\eta)^2}/h$ and $f_n(\theta,\psi) = -hk_n\cos(\theta+\psi)$. The number of stationary points of f_n depends on the values of ψ and Fr.

When $Fr < Fr_n$, the function f_n has two stationary points for $\psi < \psi_n$. Each of these can be identified with a system of transverse or divergent waves. The half-angle of the wave pattern, ψ_n, increases from $19°28'$ to $\frac{\pi}{2}$ as Fr goes from zero to Fr_n. This angle then decreases as $\sin^{-1}(Fr_n/Fr)$ when $Fr > Fr_n$. Also, when $Fr > Fr_n$, there exists only one stationary point which corresponds to the divergent waves. In this case, the source is travelling faster than the fastest waves of the n mode, and transverse waves are not possible for this steady-state problem. Since $Fr_1 > Fr_2$, the surface and internal wave patterns can be classified into three different regimes with respect to Fr. When $Fr < Fr_2$, the wave system due to each mode contains both transverse and divergent waves. When $Fr_2 < Fr < Fr_1$, the wave system due to the surface wave mode still contains both transverse and divergent waves, but the wave system due to the internal wave mode has only divergent waves. As Fr increases past Fr_1, both wave systems now contain only divergent waves.

As an example, Figs. 3-8 illustrate how the surface and internal wave patterns vary as Fr increases from a value less than Fr_2 to a value greater than Fr_1. The physical parameters are: $h_1/h = 0.5$, $\gamma = 0.5$, and corresponding to these parameters, $Fr_1 = 0.924$ and $Fr_2 = 0.383$. The source is located in the middle of the upper layer, i.e., $\zeta/h = 0.25$. In these figures, the scales in the vertical direction are stretched for clarity, and the scale factors are given in the captions. Also, the nondimensional $\bar{\zeta}^{(m)}$ is defined as $\zeta^{(m)}/h$. Figs. 3 and 4 show the surface and internal waves for $Fr = 0.37 < Fr_2$. In this case, both the surface and internal wave modes contain transverse and divergent waves, and the coupling effect can be clearly seen on the free surface where the amplitude of the surface waves due to the internal wave mode are comparable to that due to the surface wave mode. Figs. 5 and 6 show the surface and internal waves for $Fr_2 < Fr = 0.5 < Fr_1$. At this Froude number, the internal wave mode only has divergent waves. The transverse waves on the interface in Fig. 6 are due to the surface wave mode. Figs. 7 and 8 show the surface and internal waves for $Fr = 1.3 > Fr_1 > Fr_2$. Here, only divergent waves are present since the Froude number is greater than the critical Froude numbers of both modes. These and other features of the flow will be further discussed at the Workshop.

References

[1] Hudimac, A. A., "Ship Waves in a Stratified Ocean," Journal of Fluid Mechanics, Vol. 11, 1961.

[2] Sabunçu, T., "The Theoretical Wave Resistance of a Ship Travelling Under Interfacial Wave Conditions," Norwegian Ship-Model Experiment Tank, Trondheim, Pub. No. 63, 1961.

[3] Sturova, I. V., "Effect of Internal Waves on the Hydrodynamical Characteristics of a Submerged Body," Izvestiya RAN, Fizika Atmosfery i Okeana, Vol. 29, No. 6, 1993 (in Russian).

[4] Miloh, T., Tulin, M. P., and Zilman, G., "Dead-Water Effects of a Ship Moving in Stratified Seas," Proceedings of the 11th Intl. Conf. on OMAE, Vol. 1, Part A, 1992.

[5] Yeung, R. W., "Sinkage and Trim in First-Order Thin Ship Theory," J. of Ship Reseach, Vol. 16, No. 1, 1972.

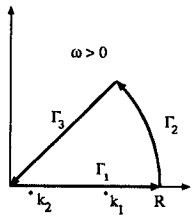

Figure 1: Integration Contour for $\omega > 0$

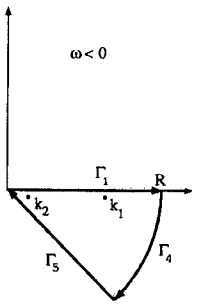

Figure 2: Integration Contour for $\omega < 0$

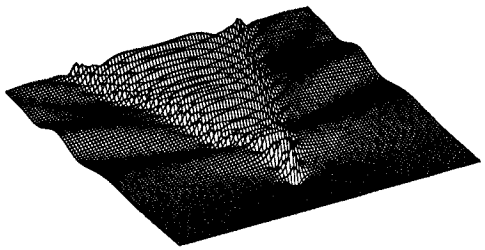

Figure 3: Surface Waves,$4E4 \times \bar{\zeta}^{(1)}, Fr = .37$

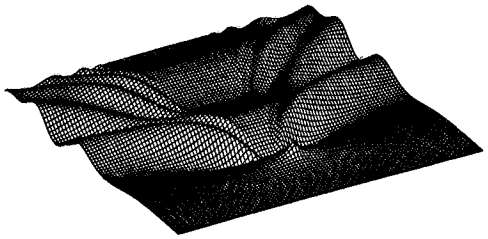

Figure 4: Internal Waves,$3E4 \times \bar{\zeta}^{(2)}, Fr = .37$

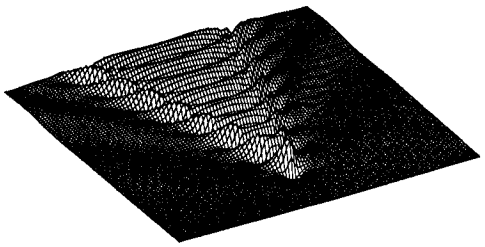

Figure 5: Surface Waves,$4E4 \times \bar{\zeta}^{(1)}, Fr = .5$

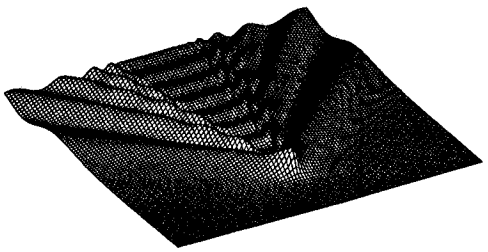

Figure 6: Internal Waves,$6E4 \times \bar{\zeta}^{(2)}, Fr = .5$

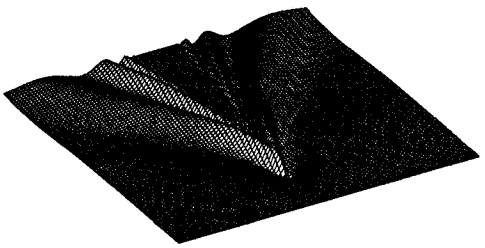

Figure 7: Surface Waves,$7E4 \times \bar{\zeta}^{(1)}, Fr = 1.3$

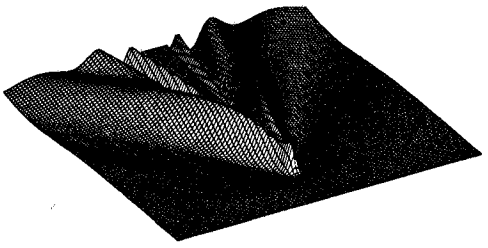

Figure 8: Internal Waves,$3E5 \times \bar{\zeta}^{(2)}, Fr = 1.3$

DISCUSSION

Kuznetsov N.: Have you any physical explanation of phase shift for internal waves?

Nguyen T., Yeung R.W.: The amplitudes of the surface waves and internal waves due to the surface wave mode are in phase, but the amplitudes are 180° out-of-phase for the internal wave mode. This situation is similar to the oscillations of two point masses connected by linear, elastic springs and suspended in a vertical plane. In the first mode of vibration at the natural frequency ω_1, the masses move together and their oscillations are in phase. In the second mode of vibration at frequency ω_2, the masses move in opposite directions and their displacements are 180° out-of-phase.